Support information

Efficient oxygen evolution activity for heterojunctions CoFe-PBA using a bimetallic probe (Mo/Cu) at room temperature: construction of multilayered activated structural bodies and cationic vacancies

Lihai Wei[1], Zhihao Liu[1], Xiaodong Wu[2, *], Huabo Huang[3, *], Qianqian Jiang[1, *], Jianguo Tang[1, *]

[1] Institute of Hybrid Materials, National Center of International Research for Hybrid Materials Technology, National Base of International Science & Technology Cooperation, College of Materials Science and Engineering, Qingdao University, Qingdao, 206000, P. R. China

[2] College of Materials Science and Engineering, Nanjing Tech University, Nanjing, 210009, P. R. China

[3] Hubei Key Laboratory of Plasma Chemistry and Advanced Materials, School of Materials Science and Engineering, Wuhan Institute of Technology, Wuhan 430205, China.

E-mail: kaiqian2008@qdu.edu.cn, wuxiaodong@njtech.edu.cn, hbhuang@wit.edu.cn and tang@qdu.edu.cn.

1. Experimental methods

1.1 Catalyst preparation

Chemicals: ammonium molybdate tetrahydrate ($(NH_4)_6Mo_7O_{24}•4H_2O$) was purchased from Sinopharm; copper chloride dihydrate ($CuCl_2•2H_2O$) was purchased from Sinopharm; cobalt hexahydrate and nitrate ($Co(NO_3)_2•6H_2O$) was purchased from Aladdin; potassium ferrocyanide ($K_3[Fe(CN)_6]$) was purchased from Aladdin; trisodium citrate hexahydrate ($Na_3C_6H_5O_7•2H_2O$) was purchased from Sinopharm .

Mo/CoFe-PBA solution: 0.08 mmol of $(NH_4)_6Mo_7O_{24}•4H_2O$, 0.4 mmol of $Co(NO_3)_2•6H_2O$, 0.2 mmol

of $K_3[Fe(CN)_6]$, and 0.4 mmol of $Na_3C_6H_5O_7•2H_2O$ were placed into 30 mL of deionized water with ultrasonic stirring.

Preparation of Mo/CoFe-PBA@IF 1•1.2 cm^2 of iron foam (IF) was immersed in the previously prepared Mo/CoFe-PBA solution for 8 hours (labeled as Test Tube 1). Remove and freeze-dry.

Cu/CoFe-PBA solution: 0.6 mmol $CuCl_2·2H_2O$, 0.4 mmol $Co(NO_3)_2•6H_2O$, 0.2 mmol $K_3[Fe(CN)_6]$, and 0.4 mmol $Na_3C_6H_5O_7•2H_2O$ in 30 mL of deionized water with ultrasonic stirring.

Preparation of Cu/CoFe-PBA@IF 1•1.2 cm^2 of iron foam (IF) was immersed in the previously prepared Cu/CoFe-PBA solution for 8 hours (labeled as Test Tube 2). Remove and freeze-dry.

CoFe-PBA configuration: 0.4 mmol $Co(NO_3)_2•6H_2O$, 0.2 mmol $K_3[Fe(CN)_6]$ and 0.4 mmol $Na_3C_6H_5O_7•2H_2O$ were placed in 30 ml of deionized water and sonicated.

Preparation of CoFe-PBA@IF 1•1.2 cm^2 of iron foam (IF) was immersed in the previously prepared CoFe-PBA solution for 8 hours (labeled as Test Tube 3). Remove and freeze-dry.

Preparation of Cu/Fe-PBA solution: 0.06 mmol $CuCl_2·2H_2O$, 0.2 mmol $K_3[Fe(CN)_6]$ and 0.4 mmol $Na_3C_6H_5O_7•2H_2O$ were placed in 30 ml of deionized water and sonicated.

Preparation of Cu/Fe-PBA@IF 1•1.2 cm^2 of iron foam (IF) was immersed in the previously prepared Cu/Fe-PBA solution for 8 hours (labeled as Test Tube 4). Remove and freeze-dry.

Preparation of Mo/Fe-PBA solution: 0.08 mmol$(NH_4)_6Mo_7O_{24}•4H_2O$, 0.2 mmol $K_3[Fe(CN)_6]$ and 0.4 mmol $Na_3C_6H_5O_7•2H_2O$ were placed in 30 ml of deionized water and sonicated.

Preparation of Mo/Fe-PBA@IF 1•1.2 cm^2 of iron foam (IF) was immersed in the previously prepared Mo/Fe-PBA solution for 8 hours (labeled as Test Tube 2). Remove and freeze-dry.

1.2 Electrochemical measurements

Electrochemical tests were carried out using a conventional three-electrode system where Cu/CoFe-

PBA@IF and Mo/CoFe-PBA@IF with a cross-sectional area of 1 cm^2 were used as working electrodes, platinum was used as the counter electrode, glycerol/mercury oxide was used as the reference electrode (for electrochemical tests), and the electrolyte was a 1M KOH solution. An electrochemical workstation (CHI660E, Shanghai Chenhua Instrument Co., Ltd.) was used for instrumentation.

Electrochemical studies were performed in a standard three-electrode system with 80% IR-compensated linear scanning voltammetry (LSV) measurements at 20 $mV \cdot S^{-1}$. The Tafel slope was measured by the Tafel equation $\eta = b \times \log(j/j_0)$, where η is the 80% IR-compensated OER overpotential, b is the Tafel slope, and j0 is the exchanged current density. The EIS was studied over the frequency range of 1-100,000 Hz. The ECSA was analyzed by the CV period of the Faraday current region and the double layer capacitance (C_{dl}) value in terms of $ESCA = C_{dl}/C_s$. The C_s value is 40. The overpotential (η) measured by OER is based on the Nernst equation: $E(RHE)=E(Hg/HgO)+0.0591\times pH+0.098$, and then calculated by the following equation: $\eta=E(RHE)-1.23V$.

1.3 Laboratory Instruments.

Table S1 Scientific instruments and code numbers and manufacturers involved in the experimental synthesis.

Instrument	Instrument Code No.	Manufacturer
electronic balance	FA1004B	Shanghai Keping Instrument Co.
Xiangyi High-Speed Tabletop Centrifuge	H1850R	Changsha Xiangyi Centrifuge Instrument Co.

Freezing vacuum drying oven	DZF	Beijing Guangming Medical Instrument Co.
ultrasonic cleaner	KQ3200DA	Kunshan Ultrasonic Instrument Co.
Electrochemical workstation	CHI660E	Shanghai Chenhua Instrument Co.

Table S2. Scientific instruments and code numbers and manufacturers involved in the physical and chemical characterization of experimental samples.

Instrument	Instrument Code No.	Manufacturer
Field Emission Scanning Electron Microscopy	JSM-7800F	Nippon Electronics Corporation
transmission electron microscope	JSM-2100Plus	Nippon Electronics Corporation
X-ray photoelectron spectrometer	PHI5000 Versaprobe III	Nippon Electronics Corporation
X-ray diffractometer	Ultima IV	Japanese science

1.4 Turnover frequency (TOF) calculations

The resulting variation of TOF versus voltage V is shown in Figure S11

The TOF (s^{-1}) value was calculated by cyclic voltammetry (CV) measurement of the quantitative number of active sites (n). Specifically, the n value for the prepared catalyst is calculated as follows[1, 2]:

$$n = \frac{Q}{2F} = \frac{It}{2F} = \frac{IV}{2F\mu}$$

Q is the voltammetric charge, F stands for the Faraday constant ($C \cdot mol^{-1}$), I stands for the current (A), t is the time (s), V refers to the voltage (V) and μ is the employed scan rate ($V \cdot s^{-1}$). Therefore, the original formula for TOF is as follows:

$$TOF=\frac{I}{mnF}$$

where I stands for current (A) and V refers to voltage (V), so IV can be replaced by CV integral fitting area. So the formula for TOF is as follows:

$$TOF=\frac{I\mu}{2IV}$$

1.5 A recent study of the comparative oxygen precipitation properties of PBA.

Table S3. Comparative studies of recent PBA oxygen precipitation properties (active substance, overpotential, tafel, and literature sources).

Active substance	OER overpotential（10 mA•cm^{-2}）	Tafel slope	Reference
（Cu/CoFe-PBA@IF）	265 mV	50.8 mV•dec^{-1}	this article
（Mo/CoFe-PBA@IF）	267 mV	41.6 mV•dec^{-1}	this article
Fe-Co_xP	300 mV	49 mV•dec^{-1}	[3]
$CoSe_2$ NBs	335 mV	54.2 mV•dec^{-1}	[4]
Ar-CoFe PBA	305 mV	36.1 mV•dec^{-1}	[5]
O-PBA/N-CNT	280 mV	48 mV•dec^{-1}	[6]
CoNi-PBA-2	280 mV	63 mV•dec^{-1}	[7]
CoFeZn-PBA	343 mV	75 mV•dec^{-1}	[8]
CoB@300	290 mV	62 mV•dec^{-1}	[9]
Co/Mn-ZIF@Fe-Co-Mn	270 mV	78 mV•dec^{-1}	[10]

2. Pictures of relevant test data.

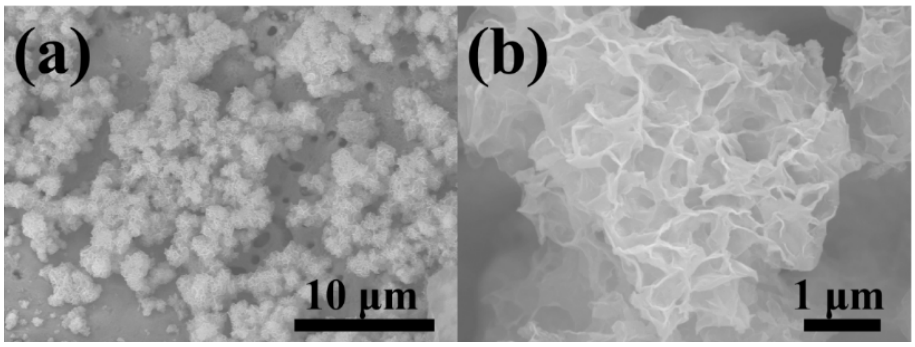

Figure S1. Mo/CoFe-PBA@IF of a) SEM image and b) individual morphology magnification.

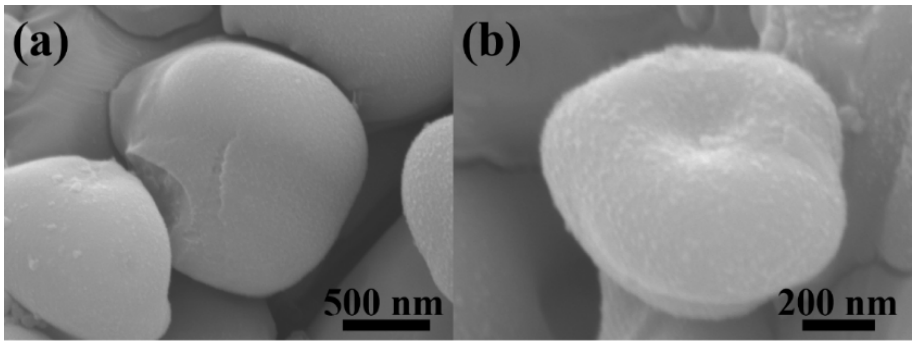

Figure S2. CoFe-PBA@IF of a) SEM image and b) individual morphology magnification.

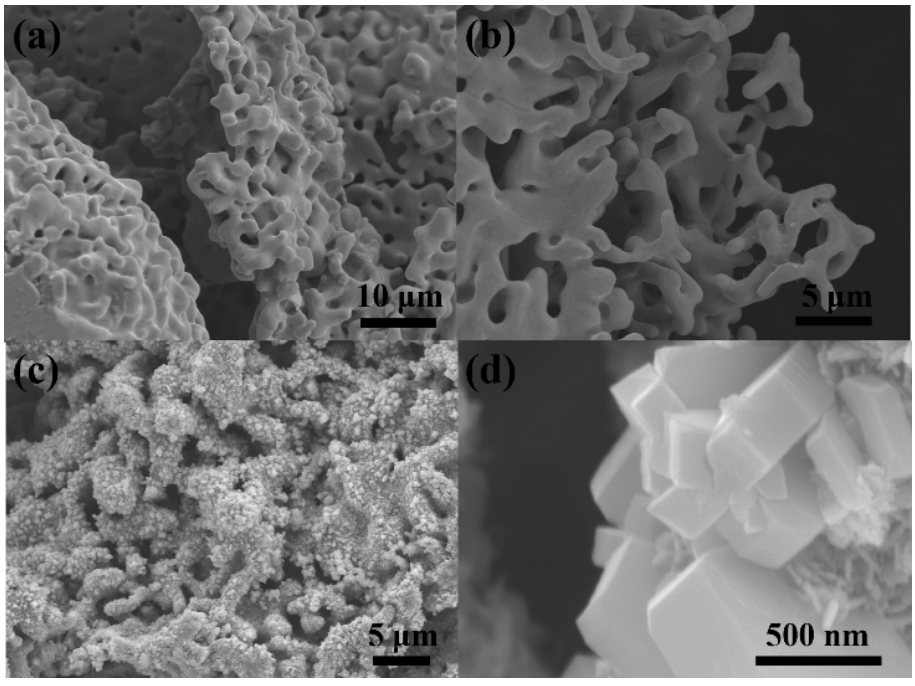

Figure S3. SEM images of (a and b) Mo/Fe-PBA@IF and (c and d) Cu/Fe-PBA@IF.

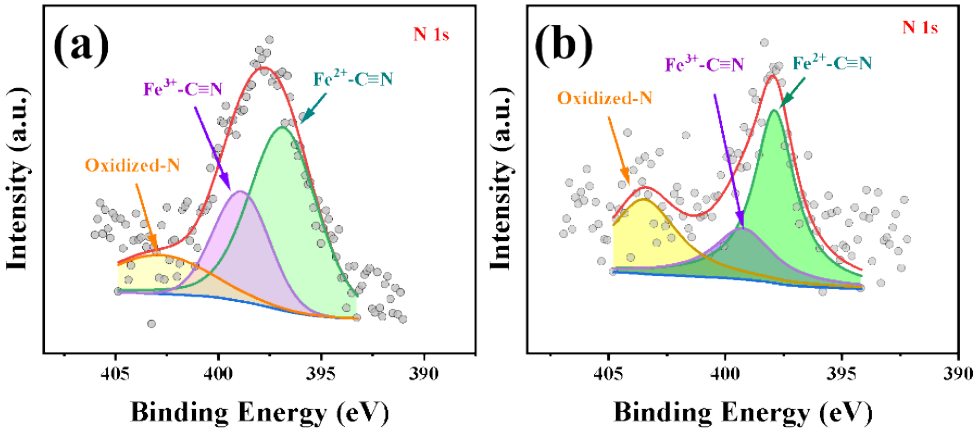

Figure S4. XPS images of a) Mo/CoFe-PBA@IF and b) N1s in Cu/CoFe-PBA@IF.

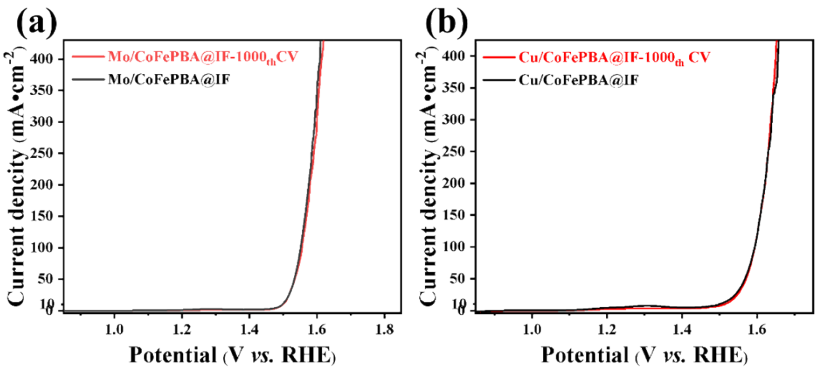

Figure S5. a) LSV images of Mo/CoFe-PBA@IF and b) Cu/CoFe-PBA@IF before and after the 1000th CV cycle.

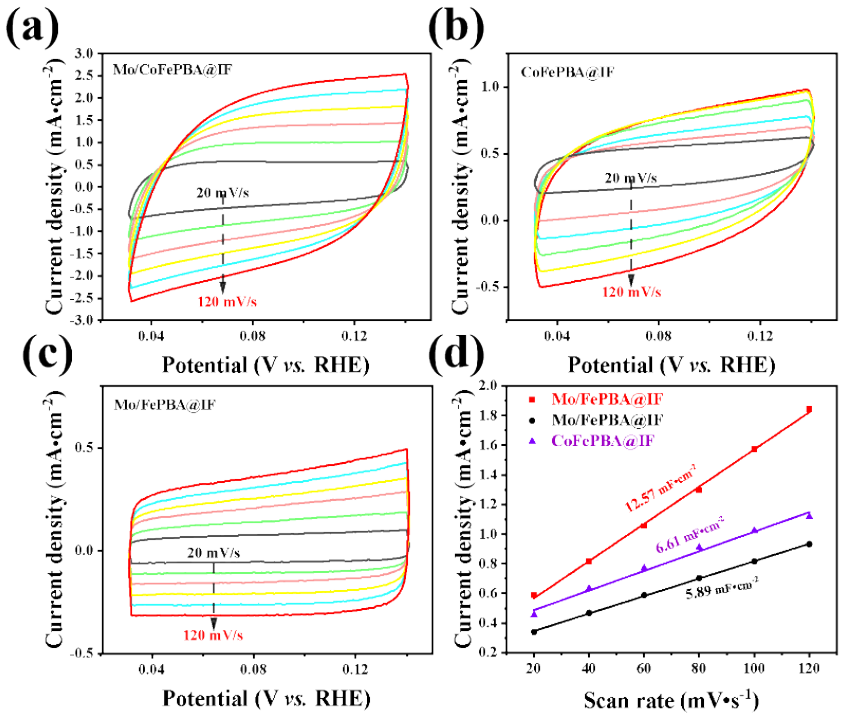

Figure S6.a) Mo/CoFe-PBA@IF, b) CoFe-PBA@IF, c) CV curves of Mo/Fe-PBA@IF at different sweep speeds and d) Capacitance current density as a function of scan rate for Mo/CoFePBA@IF, Mo/FePBA@IF, and CoFePBA@IF.

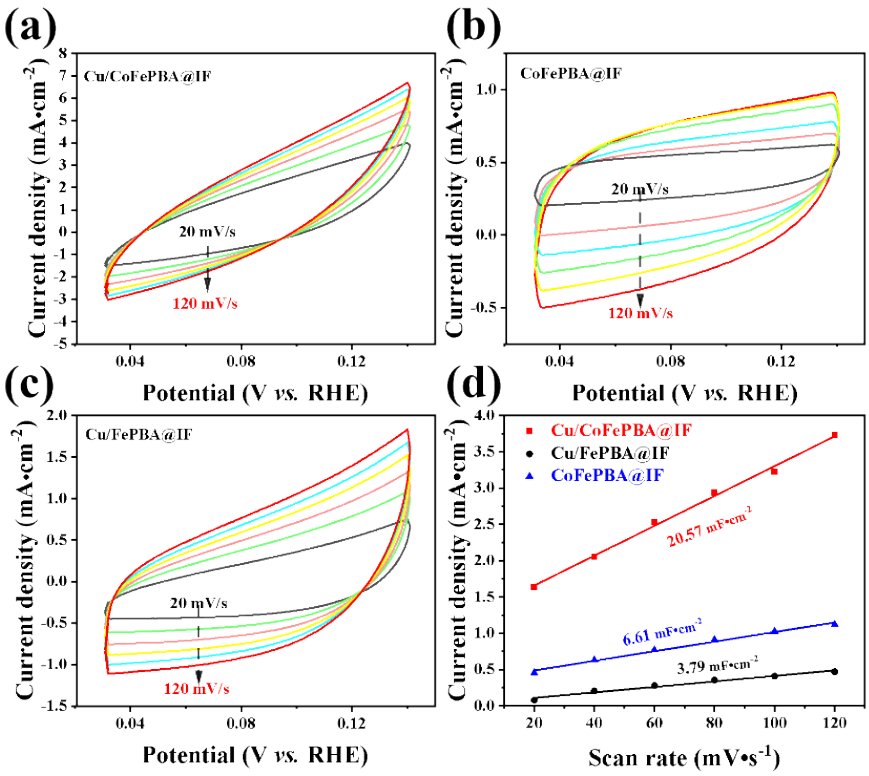

Figure S7.a) CV curves of Cu/CoFe-PBA@IF, b) CoFe-PBA@IF, c) Cu/Fe-PBA@IF at different sweep speeds and d) double layer capacitance (C_{dl}) curves.

Table S4. Adsorption Gibbs free energy for *OH, *O and *OOH intermediates and Gibbs free energy for each elementary step during OER for different kinds of structures.

	$\triangle G_{OH*}$	$\triangle G_{O*}$	$\triangle G_{OOH*}$	$\triangle G1$	$\triangle G2$	$\triangle G3$	$\triangle G4$
Cu site	2.089	4.184	4.870	2.089	**2.095**	0.686	0.049
Co site	1.555	2.827	4.627	1.555	1.272	**1.800**	0292
Fe site	0.458	1.611	3.504	0.458	1.153	**1.893**	1.415

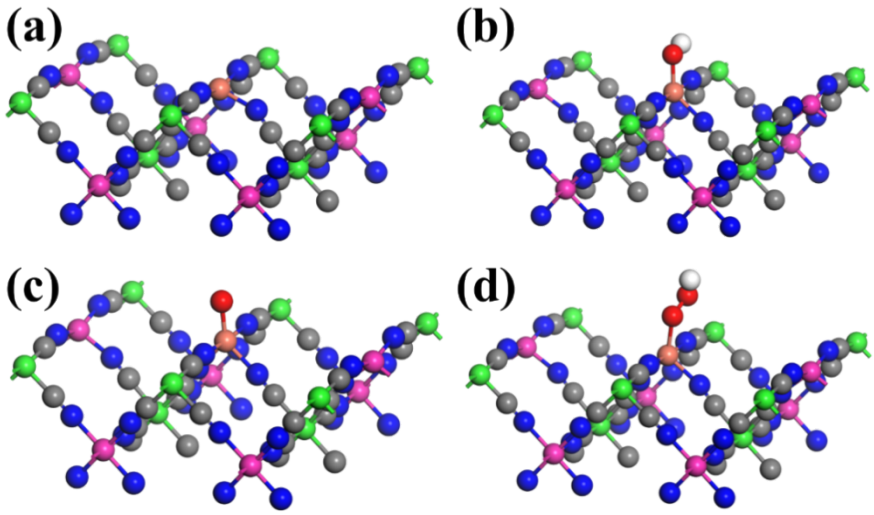

Figure S8. Adsorption of (a) Cu/CoFe-PBA@IF (4 4 0) on the surface of (b) *OH, (c) *O, and (d) *OOH constructed with Cu as the active site. (Cu atoms in orange, Co atoms in pink, Fe atoms in green, C atoms in gray, N atoms in blue, and O atoms in red).

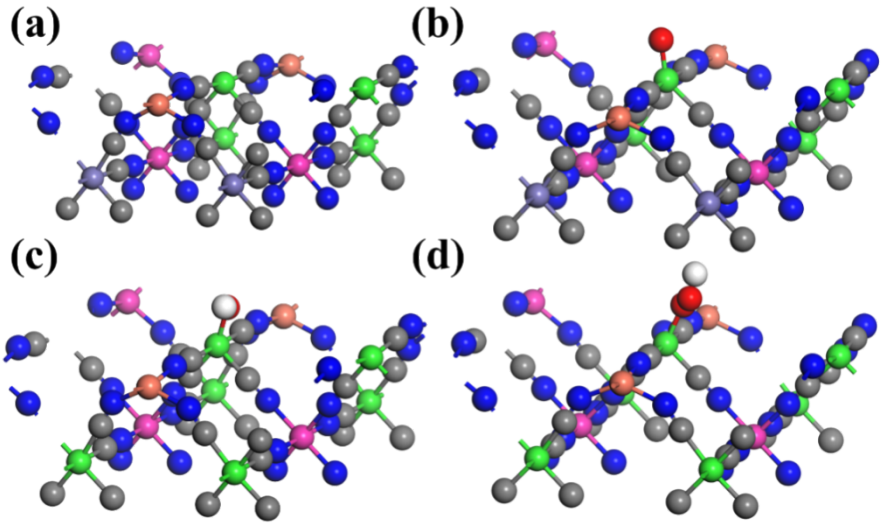

Figure S9. Adsorption of (a) Cu/CoFe-PBA@IF (4 4 0) on the surface of (b) *OH, (c) *O, and (d) *OOH constructed with Fe as the active site. (Cu atoms in orange, Co atoms in pink, Fe atoms in green, C atoms in gray, N atoms in blue, and O atoms in red).

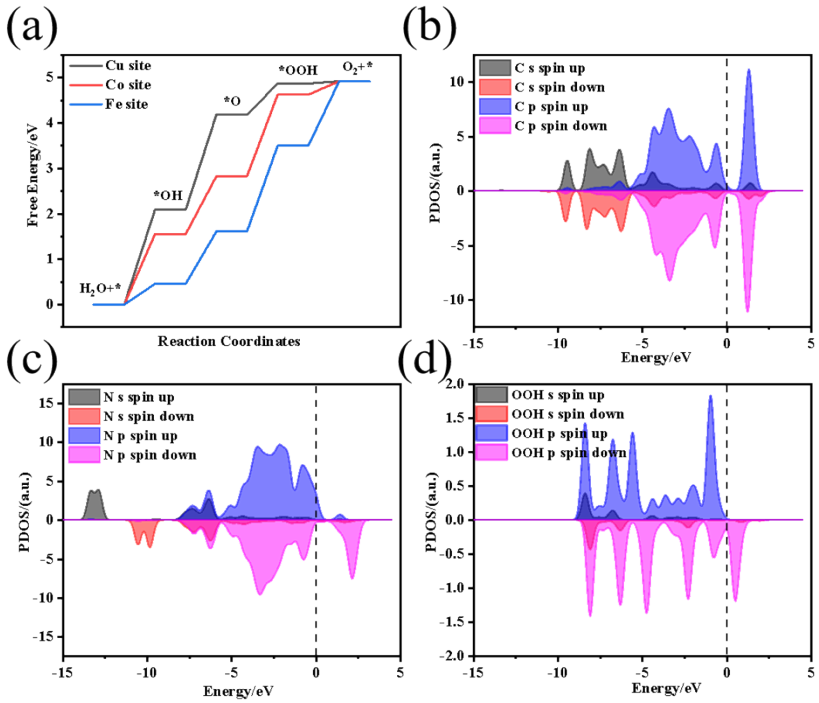

Figure S10. (a) Gibbs free energy step diagram at U = 0 V; (b-d) partial density of states distributions for C, N, and OOH.

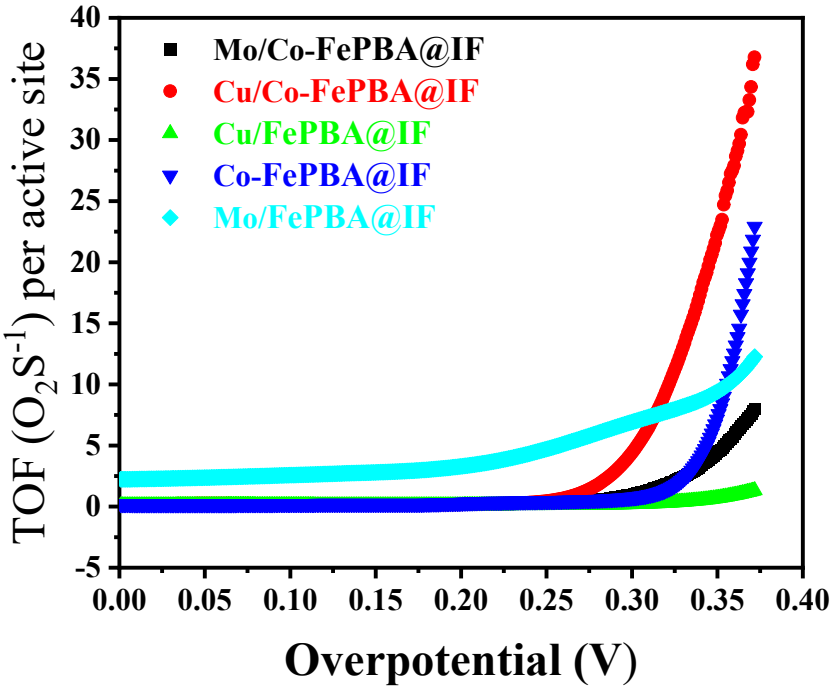

Figure S11. Transformation frequencies (TOF) of Cu/CoFe-PBA@IF, Mo/CoFe-PBA@IF, CoFe-PBA@IF, Cu/Fe-PBA@IF Mo/Fe-PBA@IF.

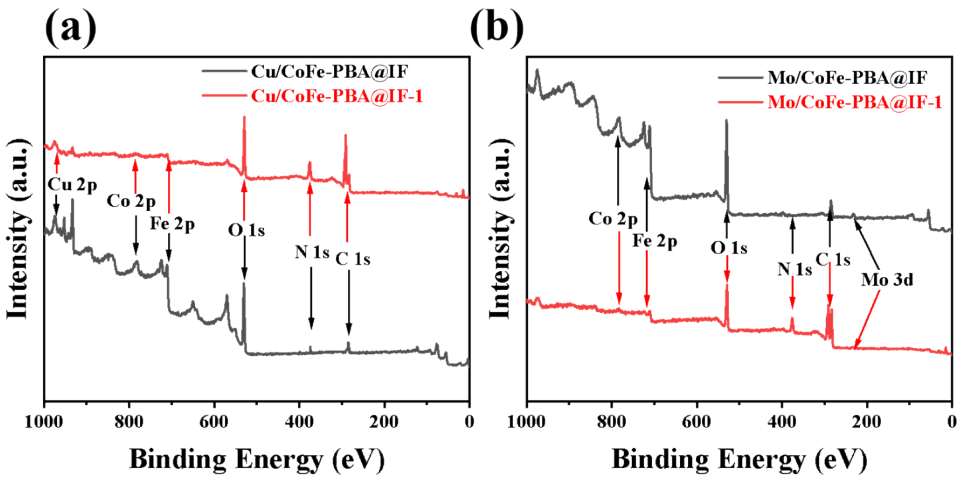

Figure S12. Full XPS spectra of (a) Cu/CoFe-PBA@IF and (b) Mo/CoFe-PBA@IF before and after the OER reaction (Cu/CoFe-PBA@IF-1 and Mo/CoFe-PBA@IF-1 represent post-reaction XPS).

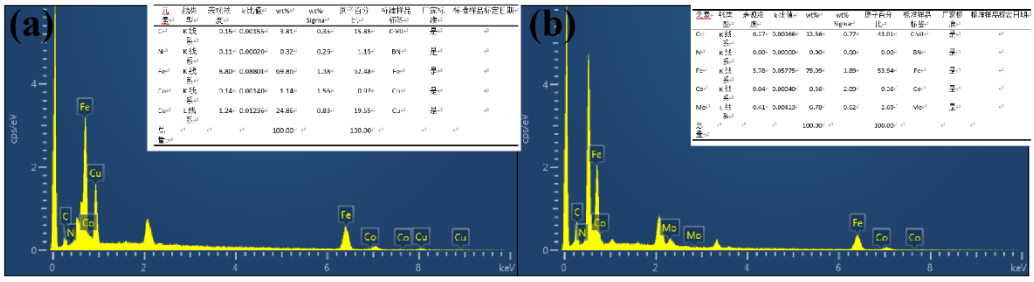

Figure S13. Elemental content concentration analyses of (a) Cu/CoFe-PBA@IF and (b) Mo/CoFe-PBA@IF (face swept).

3. Reference

1 Y. Tang, Q. Liu, L. Dong, H. B. Wu and X.-Y. Yu, *Applied Catalysis B: Environmental*, 2020, **266**, 118627.

2 P. Wang, J. Zhu, Z. Pu, R. Qin, C. Zhang, D. Chen, Q. Liu, D. Wu, W. Li, S. Liu, J. Xiao and S. Mu, *Applied Catalysis B: Environmental*, 2021, **296**, 120334.

3 W. Song, X. Teng, Y. Niu, S. Gong, X. He and Z. Chen, *Chem. Eng. J.*, 2021, **409**, 128227.

4 V. Ganesan and J. Kim, *Mater. Lett.*, 2018, **223**, 49-52.

5 F. Diao, M. Rykær Kraglund, H. Cao, X. Yan, P. Liu, C. Engelbrekt and X. Xiao, *Journal of Energy Chemistry*, 2023, **78**, 476-486.

6 S. Aulia, Y.-C. Lin, L.-Y. Chang, Y.-X. Wang, M.-H. Lin, K.-C. Ho and M.-H. Yeh, *ACS Applied Energy Materials*, 2022, **5**, 9801-9810.

7 M. Ren, J. Lei, J. Zhang, B. I. Yakobson and J. M. Tour, *ACS Appl. Mater. Interfaces*, 2021, **13**, 42715-42723.

8 H. Zou, X. Liu, K. Wang, Y. Duan, C. Wang, B. Zhang, K. Zhou, D. Yu, L.-Y. Gan and X. Zhou, *Chem. Commun.*, 2021, **57**, 8011-8014.

9 R. K. Tripathy, A. K. Samantara and J. N. Behera, *Dalton Trans.*, 2022, **51**, 2782-2788.

10 Q. Zhang, H. Wang, W. Han, L. Yang, Y. Zhang and Z. Bai, *Nano Research*, 2023, **16**, 3695-3702.